Thermal modelling of the discharge of a 180kW.h latent thermal energy storage demonstrator

Amandine da Col, Fabrice Bentivoglio, Benoît Stutz

ENERSTOCK 2024
The 16th IAE EST CP International Conference on Energy Storage
June 5–7, 2024
Lyon, France

Thermal modelling of the discharge of a 180kW.h latent thermal energy storage demonstrator

Amandine Da Col[1,2], Fabrice Bentivoglio[2,*], Benoît Stutz[2]
1 Univ. Grenoble Alpes, CEA, LITEN, DTCH, 38000 Grenoble, France
2 Université Savoie Mont-Blanc, LOCIE Laboratory, UMR 5271, CNRS, 73370 Le Bourget-du-Lac, France
*Corresponding author e-mail: fabrice.bentivoglio@cea.fr

Abstract

This paper presents a comparison between numerical and experimental results for the discharge of a 180 kWh latent thermal energy storage. The numerical model has been presented and validated for different charging cases in a previous paper. It is a 1.5D model with a 1D homogeneous approach for the heat transfer fluid combined with a 1.5D approach for the phase change material. The heat transfer fluid used is water and the phase change material is RT70HC. The paper focus on the modelling of the phase-change during discharges, as the RT70HC has two solidification peaks. The model reproduces the total energy unloaded during a discharge with an accuracy of 95% and a root-mean-square error of 3 kW on outlet power.

Keywords: Numerical modelling, Thermal energy storage, Phase-change material, System-scale

Introduction

District heating networks (DHN) are an interesting solution to reduce CO2 emissions of buildings in dense areas by providing them a way to better integrate decarbonized heat (Schmidiger and al., 2020). The main challenges resides in the shift between production and demand, and in the management of the consumption peaks in the morning and evening due to domestic hot water and heating (Martinez, 2022). Currently, they are mainly managed using fossil fuel boilers.

Thermal Energy Storage (TES) are a key component to better manage these peaks. It could smooth the urban heating network load by charging when the demand is low and supplying during peak demand. Thus, renewable energy systems like biomass, heat pumps or geothermal energy could more often operate in conditions closer to nominal conditions, gaining life-expectancy and efficiency (Guelpa and Verda, 2019). In addition, renewable and intermittent sources like wasted heat or waste incineration could be better exploited by storing their production during periods of low demand instead of sometimes being lost.

Among the different technologies developed for DHN, latent heat TES allows to store energy with a high density. It is particularly adapted in urban areas where space is generally limited.

This paper presents the validation of a numerical model of a Latent Heat TES (LHTES) against experimental data coming from a large scale demonstrator. The numerical model has been previously presented and validated for different charging cases (Da Col and al, 2023). The present paper focuses on the discharging mode. This model aims to be a fast and precise tool for future design of latent heat thermal energy storages, reducing the need for computer-demanding CFD studies.

Methodology

A numerical 1.5D model has been developed on the DYMOLA software. It simulates a 180 kWh LHTES demonstrator based on shell-and-tubes technology with monophasic water as heat transfer fluid (HTF), RT70HC as the phase-change material (PCM) and aluminium fins to enhance the conductive heat transfer in the PCM. The flow inside the tubes is annular to enhance the convective heat transfer and ensure being in a forced convection laminar flow regime. A more detailed description of the demonstrator (geometry, thermocouples positions...) can be found in Bentivoglio and al (2021).

31 charge and discharge tests have been carried out on the demonstrator during the experimental campaign. In discharging mode, the cold water enters the bottom of the system by a collector. A shattering plate ensures that the flow is sufficiently distributed inside the collector to reduce the disparity of the mass flowrate between the 367 tubes.

The DYMOLA model is based on a 1D model to simulate the HTF and a conductive 1.5D model to represent the steel tube, the radial aluminium fins and the free PCM. CFD simulations are used to feed the

DYMOLA model with reduced data for the equivalent material composed by the PCM and the radial fins.

The heat exchange between the HTF and the tube is determined by the correlation from Muzychka and Yovanovich (2004). It takes into account the entrance region with an asymptotic model and is adapted to an annular fluid section.

The numerical results are compared to experimental data at macroscopic (power and energy) and local (outlet temperature and PCM temperatures) scales.

Da Col and al. (2023) concluded that the key parameters of the model are the discretization of the collectors, the convection heat transfer coefficient between the HTF and the tube, and the PCM thermal capacity model. Thus, one of the main challenges of the discharge case is to investigate the solidification behaviour of the RT70HC. Several tests had showed that this PCM has two distinct solidification plateaus. Jadal (2020) demonstrated that it is because two different species composed the material. Then, DSC tests were run in order to construct a numerical model of the material in solidification for the DYMOLA model, with the same method previously used in Da Col and al. (2023).

Results and Discussion

Thermal capacity model

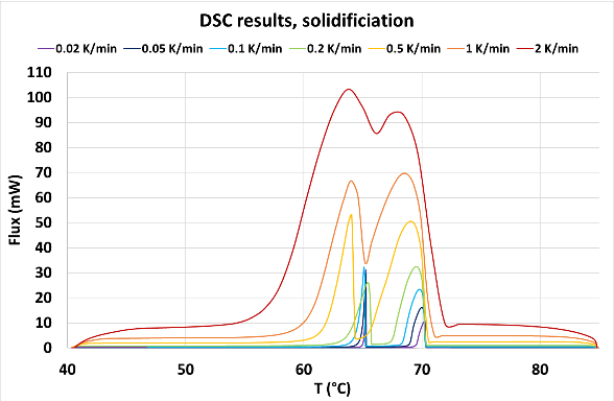

Figure 1: Differential Scanning Calorimetry results in solidification, for different temperature slopes

The DSC tests were run with temperature slopes from -0.02 K/min to 2 K/min on a same sample of 111 mg. The two phase-changes plateaus appear clearer when the solidification rate is slower. The aim was to develop a thermal capacity model that includes the two phase-changes. Integrating these results following Hu and Argyropoulos (1996) and Kahwaji and al (2021) recommendations lead to the numerical model presented in the Figure 2. It is written in the software as a table associating 8 temperatures from 50 to 80 °C to a value of thermal capacity. Between two temperature points, the software does a linear interpolation to determine the thermal capacity.

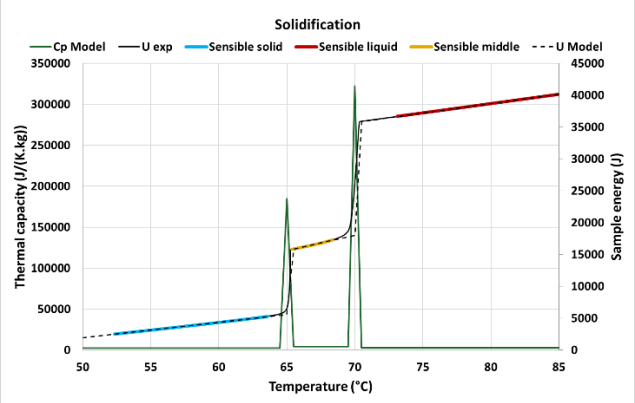

Figure 2: Numerical model for thermal capacity with integrated latent heat, based on experimental result

Constant power discharge

The first experimental case is a discharge where the mass flowrate at the bottom of the system is regulated in order to extract 25 kW from the system. Figure 3 shows the power and energy extracted from the thermal storage, calculated according to equations (1) and (2).

$$\dot{q}_{htf} = \dot{m} \times Cp_{average}(T_{in} - T_{out}) \quad (1)$$

$$q = \int_0^t \dot{q}_{htf}\, dt \quad (2)$$

At first, the power is superior to this value because of the minimum mass flowrate of the pump. After 2 hours of operation, the flow control adjusts the extracted power to the set point. After 5h30 of operation, the maximum flowrate is reached and it is no longer possible to adjust the extracted power to the setpoint.

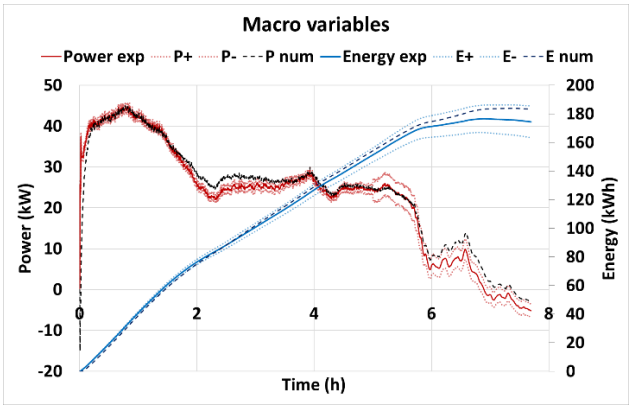

Figure 3: Power and energy extracted, with uncertainties range, with constant power discharge

The results of the comparison between the model and the experimental points are presented in the Figure 3, the Figure 4 and the Figure 6. Globally the results are in very good agreement. The root-mean-square (RMS)

error between experimental and numerical results is 2.96 kW for thermal power, and the difference in total energy extracted is 8.17 kWh, i.e. 4.68 % of the total energy. The RMS error on outlet temperature, shown on Figure 4, is 1.1°C.

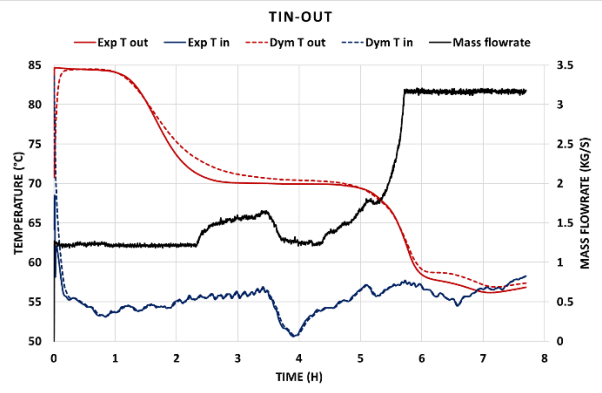

Figure 4: Inlet and outlet temperatures of the system

Locally, there is a good agreement between local and experimental results, as shown in Figure 6Figure 6. The major error is situated on "PCM2" thermocouples, the one located at the longest distance from the tube: it is probably because the model considers the edge of a cylinder with a radius of 32.2 mm whereas the real distance between the thermocouple "PCM2" and the centre of the tube is 35.45 mm, as illustrated in Figure 5. The linear thermal resistance between the edge of the fins (28.75 mm radius) and the end of the free PCM (35.45mm) is then 0.65 K/W numerically and 1.2 K/W experimentally, i.e. a difference of 54.2%.

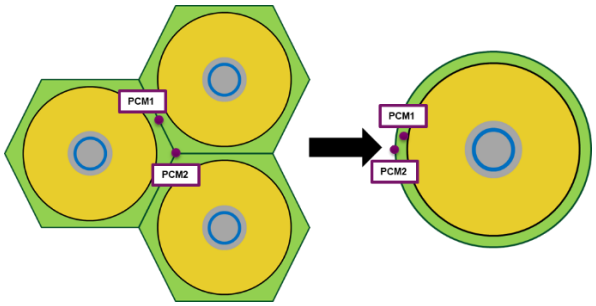

Figure 5: Positions of the thermocouples PCM1 and PCM2 in the system (left) and in the model (right)

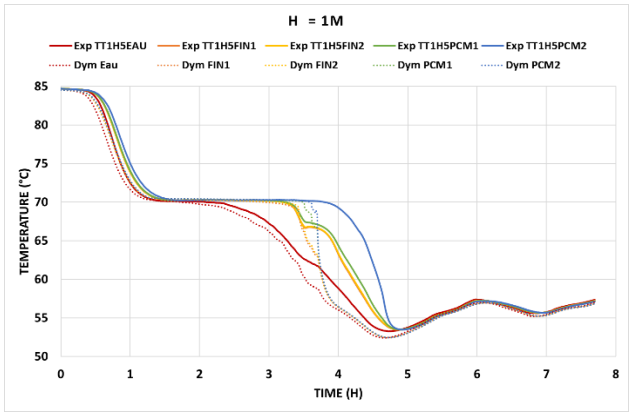

Figure 6: Local temperature of water, tube, fins and free PCM at 1 meter height

This difference does not affect much the macroscopic results nor the water temperature in the tubes, as shown in Figure 7 and Figure 7. There is a good agreement between experimental and numerical results at all levels.

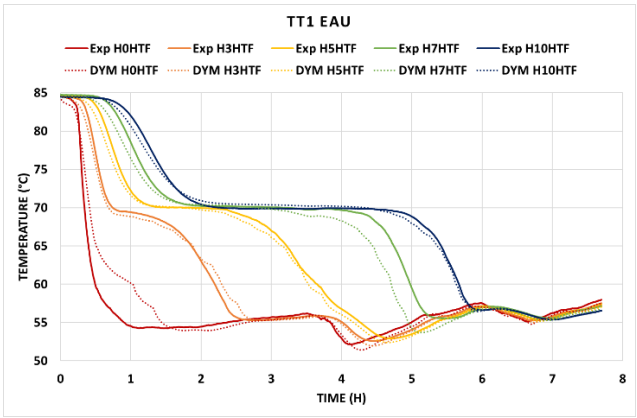

Figure 7: Water temperature inside the tube for different heights, each section being 0.5m higher than the previous, with H0 = 0m.

Constant flowrate discharge

The second experimental case is a discharge where the mass flowrate at the bottom of the system is set to 0.6 kg/s. Results are presented in Figure 8 and Figure 9.

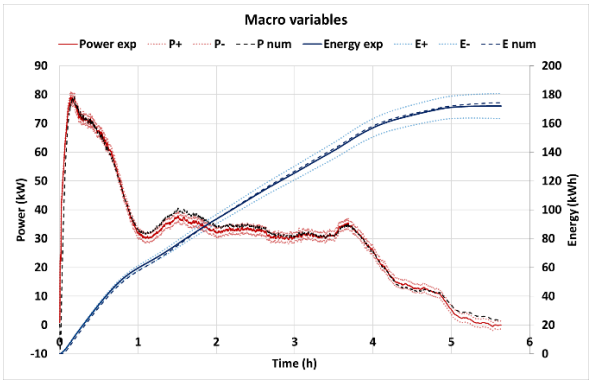

Figure 8: Macroscopic variables of the system, power and energy extracted, with uncertainties range, compared with numerical results.

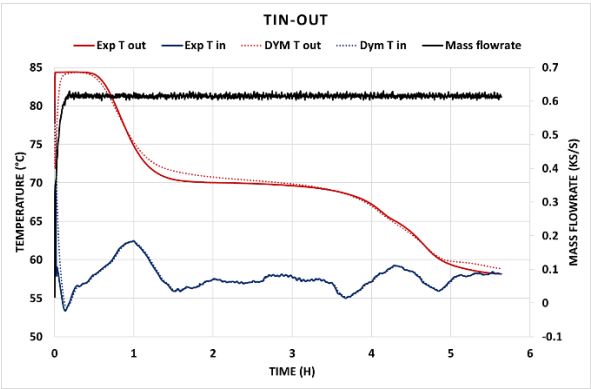

Figure 9: Inlet mass flowrate and temperature, and outlet temperature of the system

For this case, the RMS error on the power is 3.01 kW, the difference between numerical and experimental energy extracted is 2.98 kWh, i.e. 1.73 % of the total energy. The RMS error on outlet temperature is 1.62 °C.

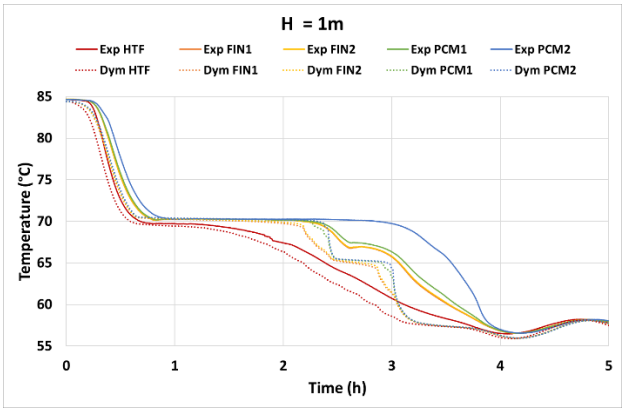

Figure 10: Local temperature in the HTF, fins zone and free PCM, at 1m height

Locally, the model reproduces the two solidifications plateaus of Figure 10 with a good agreement in terms of relative plateaus' length. This confirms that we can not neglect these two solidifications. Figure 11 illustrates the macroscopic results difference between the model that considers one solidification (1 peak) and our current model (2 peaks). Table 1 compiles the major criteria used to compare experimental and numerical data. It shows that the 1 peak model is still acceptable, but the 2 peaks model is slightly better.

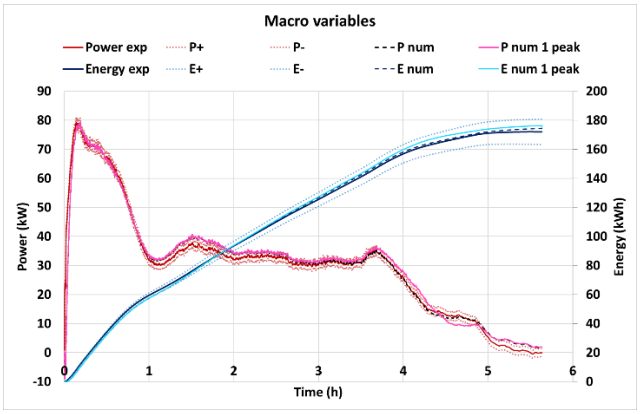

Figure 11: Macro variables, comparison between the two thermal capacity models

Table 1: Comparison between errors of the two thermal capacity models

Model	RMS on T (°C)	RMS on P (kW)	dE (kWh - %)
1 peak	1.67	3.22	3.59 – 2.08%
2 peaks	1.62	3.01	2.98 – 1.73%

Conclusions

This 1D fluid – 1.5D PCM numerical model is able to reproduce with a good agreement the experimental results for two kind of discharges, at constant flow rate and constant power. The relative error for the energy extracted is <5 %, the RMS errors on power and temperature are <3 kW and <2°C. The PCM thermal capacity model with two peaks reproduces well the thermal behaviour of the system and is an improvement compared to a model with only one peak.

This 1D fluid – 1.5D PCM model and the methodology used to determine its parameters are then validated for the charges and discharges of a latent thermal energy storage based on tube and shell technology. Thus, this method is relevant to design these systems with a reduced computer time: it requires only about 10 minutes to simulate 6 hours of operation of the whole system.

References

Bentivoglio, F. and al. (2021). Design and operation of a 180 kWh PCM heat storage at the Flaubert substation of the Grenoble urban heating network. Applied Thermal Engineering. doi.org/10.1016/j.applthermaleng.2020.116402

Da Col, A, and al. (2023). Modelling a latent heat thermal storage demonstrator and identification of the model key-parameters. Journal of Energy Storage. doi.org/10.1016/j.est.2023.109239

Guelpa, E. and Verda V. (2019). Thermal energy storage in district heating and cooling systems: A review. Applied Energy. doi.org/10.1016/j.apenergy.2019.113474

Hu, H., and Argyropoulos S.A. (1996). Mathematical modelling of solidification and melting: a review. Modelling and Simulation in Material Science and Engineering. doi.org/10.1088/0965-0393/4/4/004

Jadal, M. (2020). Caractérisation thermique d'un échangeur-stockeur constitué d'un matériau à changement de phase dans une structure conductrice.

Kahwaji, S., and al. (2021). Thermal property determination for phase change materials. The Journal of Chemical Thermodynamics 160, 106439. doi.org/10.1016/j.jct.2021.106439

Martinez, S., and al. (2022). Demand-side flexibility in a residential district: What are the main sources of uncertainty? Energy and Buildings. doi.org/10.1016/j.enbuild.2021.111595

Muzychka, Y.S., and Yovanovich, M.M. (2004). Laminar Forced Convection Heat Transfer in the Combined Entry Region of Non-Circular Ducts. Journal of Heat Transfer. doi.org/10.1115/1.1643752

Schmidiger, P., and al. (Press release, 2020). L'extension du réseau de chauffage de Saint-Louis intégrera l'EuroAirport. http://www.r-cu.fr\wp-content\uploads\2021\04\CP-Extension-reseau-chaleur-St-Louis.pdf